Investigating the n- and p-Type Electrolytic Charging of Colloidal Nanoplatelets

Emmanuel Lhuillier, Sandrine Ithurria, Armel Descamps-Mandine, Thierry Douillard, Remi Castaing, Xiang Zhen Xu, Pierre-Louis Taberna, Patrice Simon, Herve Aubin, Benoit Dubertret

Investigating the n- and p-Type Electrolytic Charging of Colloidal Nanoplatelets

Emmanuel Lhuillier,*[,†,⊥] Sandrine Ithurria,[‡] Armel Descamps-Mandine,[‡] Thierry Douillard,[§] Remi Castaing,[†] Xiang Zhen Xu,[‡] Pierre-Louis Taberna,[∥] Patrice Simon,[∥] Herve Aubin,[‡] and Benoit Dubertret*[,‡]

[†]Nexdot, 10 rue Vauquelin, 75005 Paris, France

[‡]Laboratoire de Physique et d'Etude des Matériaux, ESPCI-ParisTech, PSL Research University, Sorbonne Université UPMC Univ Paris 06, CNRS, 10 rue Vauquelin, 75005 Paris, France

[§]INSA-Lyon, UMR CNRS 5510 (MATEIS), 7 avenue Jean Capelle, 69621 Villeurbanne Cedex, France

[∥]Université Paul Sabatier, CIRIMAT/LCMIE, CNRS, 31062 Toulouse Cedex 9, France

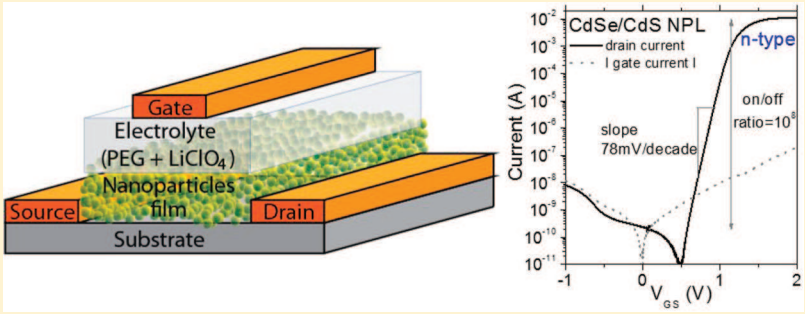

ABSTRACT: We investigate the ion gel gating of 2D colloidal nanoplatelets. We propose a simple, versatile, and air-operable strategy to build electrolyte-gated transistors. We provide evidence that the charges are injected in the quantum states of the nanocrystals. The gating is made possible by the presence of large voids into the NPL films and is sensitive to the availability of the nanocrystals surface.

1. INTRODUCTION

Nanoplatelets[1] (NPLs) are 2D colloidal materials, and the interest for this new type of colloidal nanoparticles has been mostly driven by their original optical properties. In particular, the atomic-scale control of the thickness[2,3] enables the synthesis of samples in which no inhomogeneous broadening is observed, leading to particularly narrow optical features. Thanks to this behavior, NPL appears a good candidate for optoelectronic devices with well controlled optical features. In addition, compared with 0D colloidal quantum dots (CQDs), NPL can also offer some potential improvement in charge transport. The 2D shape of NPL can lead to a larger overlap of the electron or hole wave function with neighboring NPL, while reducing the number of hopping steps to reach the electrodes thanks to their larger lateral size. The integration of NPL into transistors[4] and phototransistors[5] has recently been reported. The photoconductivity of NPL has even been shown to be enhanced by 8 decades when they are integrated with nanometer scale electrodes[6] compared with the same material operated in the hopping regime. For all of these devices, electrolyte gating was achieved through the use of ion gel electrolytes. It has been observed that this allows a fine-tuning of the conductance and photoconductance of the system. The use of ion gel gating instead of liquid electrolyte gating[7,8] was first motivated by the need for an all-solid system that allows a size reduction and thus easier integration in final devices. While the interest in electrolytic gating of NPL for optoelectronic purpose is high, the gating mechanism in films of 2D NPL still requires a deeper understanding.

Electrolyte gating was first introduced in liquid form for films of quantum dots by the Guyot-Sionnest[7,9] and Vanmaekelbergh groups.[8,10] Compared with solid-state back gating, electrolyte gating achieves a higher gate capacitance. This results from the fact that in back gating the capacitance is driven by the ratio of the dielectric contant of the gate material over the thickness of the insulating layer, which is at least a few multiples of the lattice parameter (greater than a few nanometers in practice). On the contrary, in the case of electrolytes, this is the size of the ion (<0.1 nm), rather than the electrolyte thickness, which drives the capacitance value and leads to a higher capacitance. As a consequence, while back gating remains limited to sheet densities $<10^{13}$ cm^{-2}, capacities $>10^{14}$ cm^{-2} have been obtained

DOI: 10.1021/acs.jpcc.5b05296

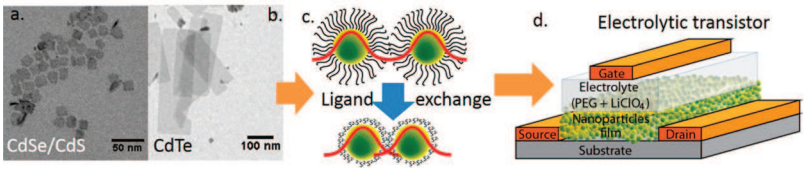

Figure 1. (a) TEM images of CdSe/CdS nanoplatelets. (b) TEM images of CdTe NPL. (c) Schematic of the ligand exchange procedure. (d) Schematic of the final electrolytic transistor.

using electrolytes.[11] The latter consequently allows injection of several charges per nanoparticle, which is generally not possible via back gating. Another key advantage for electrolyte gating is the ability to charge thick films, thanks to the percolation of ions within the film of nanoparticles. More recently, polymer and ion gel gating has been adapted to gate films of CQD,[12−15] in particular, as a probe of their doping.

We investigate the ion gel gating of NPL films. We demonstrate that this method allows fabrication of air-operable transistors with n- or p-type doping, depending on the cadmium chalcogenide compound used. The charging mechanism is further characterized by spectro-electrochemistry and impedance spectroscopy measurements. Finally, we study the effects of the physical and chemical properties (surface chemistry, film morphology, and temperature) of the films on the charging mechanism.

2. EXPERIMENTAL SECTION

2.1. Material Synthesis. *CdSe Nanoplatelets.* In a first step, cadmium(II) myristate ($Cd(Myr)_2$) is prepared following ref 16. In a typical synthesis, 240 mg of $Cd(Myr)_2$ and 25 mg Se powder are mixed in 30 mL of octadecene (ODE). The mixture is degassed under vacuum for 20 min at room temperature. Then, the atmosphere is switched to Ar, and the temperature is set to 240 °C. At 204 °C, 160 mg of cadmium(II) acetate ($Cd(OAc)_2$) is quickly added. The mixture is held for 12 min at 240 °C. One mL of oleic acid is quickly injected to quench the reaction and the solution is cooled. The NPLs are precipitated by adding ethanol. After centrifugation, the obtained solid is redispersed in hexane. The cleaning procedure is repeated three times.

CdSe/CdS Core−Shell Nanoplatelets. The procedure follows the one described by Ithurria et al. in ref 19. NPLs in hexane are transferred to *N*-methylformamide (NMFA) by the addition of sodium sulfide in NMFA ($[Na_2S] = 2g{\cdot}L^{-1}$). It is equivalent to the growth of a half layer. The CdSe-S^{2-} NPLs are then precipitated with acetonitrile to remove the excess sulfide and redispersed in NMFA. The second half layer is grown by the addition of $Cd(OAc)_2$ in NMFA. (The reaction is quasi-instantaneous.) Excess precursors are removed by precipitating the nanocrystals with a mixture of 5:1 toluene/acetonitrile. To finish the CdSe-S^{2-}-$Cd(OAc)_2$, NPLs are resuspended in NMFA. It is possible to grow several layers using Na_2S and $Cd(OAc)_2$ as precursors of sulfide and cadmium. Here the sample has 3.5 layers of CdS.

CdTe Nanoplatelets. The procedure follows the one described by Pedetti et al. in ref 17. Cadmium(II) propanoate ($Cd(Prop)_2$) is first prepared by mixing 1 g of CdO in 10 mL of propionic acid under Ar for 1 h. Then, the flask is then opened to air and the temperature is raised to 140 °C to concentrate the solution by a factor of 2. The resulting white mixture is precipitated by the addition of acetone. After centrifugation the solid is dried under vacuum for 24 h. In the glovebox, 1 M Te in tri-*n*-octylphosphine (TOPTe) is prepared by stirring 2.55 g of Te pellets in 20 mL of TOP for 4 days at room temperature. In a three-necked flask 0.13 g of $Cd(Prop)_2$, 160 μL of oleic acid, and 10 mL of ODE are degassed for 90 min at 95 °C. Then, the atmosphere is switched to Ar and the temperature is raised to 210 °C. 0.2 mL of 1 M TOPTe is quickly injected into the flask. After 20 min, the reaction is quenched by adding 1 mL of oleic acid and cooling to room temperature. Ethanol is added to precipitate the CdTe NPL. The solid obtained after centrifugation is redispersed in hexane. This procedure is repeated three times.

Additional material characterizations and details of the synthesis of other materials are given in the Supporting Information.

2.2. Device Fabrication. *Electrolyte Preparation.* The electrolyte is a mixture of polyethylene glycol (PEG), with a given molar weight (from 6×10^3 to 88×10^3 g mol^{-1}), and ions (typically $LiClO_4$). For a typical electrolyte, 50 mg of $LiClO_4$ and 230 mg of PEG (MW = 6000 g mol^{-1}) are heated together at 150 °C on a hot plate in the glovebox for 2 h.

Electrode Fabrication. Electrodes are fabricated using a regular lift-off procedure on a Si/SiO_2 wafer with an oxide thickness of 500 nm. Thermally evaporated Cr (2.5 nm) and Au (17.5 nm) are used for the contact. Electrodes are composed of 25 interdigitated pairs, which are 2.5 mm long. Two sets of electrodes have been designed with a spacing of 10 and 20 μm. The W/L ratio is 6250 for the 10 μm spaced electrodes and 3125 for the 20 μm spaced electrodes.

Ligand Exchange Procedure. The ligand exchange is done directly on the nanoparticles in solution. For a typical ligand exchange, 15 mg of Na_2S is dissolved in 0.5 mL of NMFA by sonication. Then, 1 mL of the solution of nanoparticles in a nonpolar solvent is added. The mixture is then stirred until the nanoparticles have transferred to the polar phase. Then, 2 mL of hexane is added, and after sonication, the nonpolar phase is removed. This step is repeated a second time. Finally, the nanoparticles are precipitated by the addition of acetonitrile, and after centrifugation the solid is redispersed in NMFA. For narrow band gap materials (PbS, PbSe, HgTe), the nanoparticles are dispersed in a mixture of hexane and octane (9:1 volume ratio). The electrodes are warmed at 125 °C on a hot plate for 2 min and then cooled to room temperature. The solution is drop-cast onto the interdigitated electrodes. The typical thickness for a film is 30 nm. Then, the film is dipped in a solution of Na_2S in ethanol ($1-5$ g L^{-1}) for 1 min for PbS and PbSe and 30s for HgTe. The film is then rinsed in pure ethanol. Finally, the film is annealed at 80 °C for 1 min.

Field Effect Transistor Preparation. To prepare the electrolyte transistor, we softened the electrolyte by warming it on a hot plate at 80 °C. The electrolyte is brushed on the film of nanoparticles processed with the S^{2-} ligand exchange. Typical thickness is ∼1 mm. The device is finally cooled down. Finally, a TEM grid is deposited on the electrolyte as a gate

electrode. The sample can be brought up to the measurement setup in air. Figure 1 summarizes the different steps of the preparation of the electrolytic transistor.

2.3. Characterization. XRD measurements are made using a Philips X'pert X-ray diffractometer operating at 40 kV and 40 mA with an X-ray wavelength of 1.54 Å. UV−visible spectra are acquired using a Cary 5E spectrometer. Thin films are prepared for the SEM and TEM imaging in Figure 3 using a Ga^{2+} Focus Ion Beam (NVision 40 from ZEISS). SEM images were made using the electron beam in the FIB instrument. Transmission electron microscopy images are acquired on a JEOL 2010F TEM.

Electrical measurements are performed either using a probe station operating under air or in an Oxford CFV cryostat. Bias and current measurements are made using two Keithley 2400 source meters. For the transfer curve (I_{DS} vs V_{GS}) the bias step is 1 mV and the sweep rate is 2 or 3 mV s^{-1}. Cyclic voltammetry measurements are made with a film of nanoparticles with a known mass on a ~1 cm^2 Cu substrate. A liquid electrolyte is used made of a mixture of 1 M $LiPF_6$ in a mixture of 1:1 ethylene carbonate and dimethyl carbonate. A Li counter electrode is used and the cell is connected to a multipotentiostat (VMP3 from Bio-Logic) and the bias sweep rate is 100 $\mu V \cdot s^{-1}$. For electrochemical impedance spectroscopy data, the same VMP3 setup is used. In this case a 2 V DC bias was applied and modulated by a 1 mV AC signal.

3. RESULTS AND DISCUSSION

3.1. Ion-Gel-Gated Nanoplatelet Films. To build an ion-gel-gated transistor, we first start from the NPL solution (CdSe, CdSe/CdS or CdTe) and perform a ligand exchange step[18] to S^{2-}. Early motivation for this ligand exchange was to boost the carrier mobility, but it will also impact the carrier density, as discussed later in the text. The obtained solution of NPL is then deposited on Cr/Au electrodes. Finally, a gel electrolyte is brushed onto the NPL film and a Cu metallic grid is used as top gate electrode. The procedure is described in Figure 1.

In the case of CdSe/CdS NPL, we observe a strong n-type gating. The on−off ratio can be as high as 10^8 while operating the transistor under low drain (0.5 V) and gate bias (<2 V); see Figure 2a. This current modulation is one of the highest

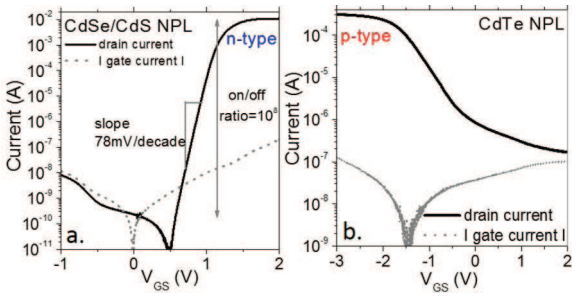

Figure 2. Transfer curve (drain current as a function of gate bias) for CdSe/CdS NPL (a) and CdTe (b) film. The gate current is also plotted to estimate the leakage current.

reported for colloidal nanocrystal films and is 1 order of magnitude higher than that for pure CdSe NPL.[4] In the off state, the system is limited by the leakage current through the electrolyte. The sub threshold slope can be as low a 78 mV/decade, which is close to the thermodynamic limit (60 mV/decade at room temperature). The difference is likely a result of filling of defect states introduced by the C-ALD procedure[20] used to grow the CdS shell.

The gating of CdTe nanocrystals has been far less investigated and was only recently observed.[20] CdTe NPL shows p-type charging; see Figure 2b. The performance is reduced compared with the CdSe/CdS film; nevertheless, the on−off ratio of 10^3 is the highest value reported for CdTe colloidal system, to the best of our knowledge.

3.2. Electrochemical Properties. One of the key advantages of our method to build the electrolytic transistor is their air operability. All of the measurements have been conducted in air, and cycling over a week (>150 cycles) barely affects the transistor performances. The thick ion gel layer probably protects the NPL film. This is a significant improvement compared with liquid electrolytic gating, which required both air-free preparation and use of the device.

The method is not limited to NPL and can be operated with a large range of nanocrystals: CdSe QD, CdS nanorods, PbS QD and cubes, PbSe QD, and HgTe QD; see Figure S10. In the following, we choose to focus on a film of CdSe/CdS NPL. We want to address how the 2D aspect of the NPL combined with the ion gel nature of the electrolyte affects the charging mechanism.

We start by performing spectroelectrochemistry on the NPL film. We follow, as a function of time and charging, the optical absorption of the NPL; see Figure 3a. The CdSe/CdS NPL absorption spectra typically present two peaks associated with the heavy-hole to conduction band ($\lambda \approx 630$ nm) and the light-hole to conduction band transition. As a function of charging, we observe a bleach of the optical features resulting from the filling of the conduction band by the injected electron. We can conclude that the nanoparticle quantum states are filled by the electrolyte gating.

The viscosity of the electrolyte combined with the 2D shape of the NPL may slow the percolation process compared with liquid electrolytes. We observe that in response to a step of gate bias the gate current typically has two time constants: one around 1 s and one around 1 min. To further characterize the dynamics of the charging, we use electrochemical impedance spectroscopy. We typically apply a 1 mV AC bias over a 2 V DC gate bias, which is above the turn on voltage of the electrolyte transistor, and measure the current, allowing the evaluation of the associated impedance and phase. At high frequency (f between 50 Hz and 1 kHz), the phase is close to 90°, which is the expected value for a pure capacitor; see Figure 3c. This behavior corresponds to the flattened half circle in the impedance plot; see Figure 3b. We can relate this behavior to the formation of the electrostatic double layer.[21] By further slowing down the dynamics, the phase drops and gets close to 0°, as expected for resistive behavior. In the impedance plot, the low frequency part of the diagram corresponds to the tail at high Re(Z). The resistive behavior is usually associated with diffusion-limited process. To model the electrochemical properties of the NPL film coupled to the ion gel electrolyte, we use the equivalent circuit[22] proposed in Figure 3b. The circuit is composed of an electrolyte resistor ($R_{el} \approx 500\Omega$) in series with a RC circuit made of a capacitor C_{DL} modeling the double-layer gating and R_{CT} which accounts for the charge-transfer resistance. To take into account that the half circle of the impedance plot is flattened we model the impedance with the expression $C_{DL} = (1/(Y_O(jw)^a))$ where $j^2 = -1$, w is the pulsation and, Y_O is the magnitude. We obtain a good fit with $\alpha = 0.8$, while $\alpha = 1$ will have described an ideal RC circuit.

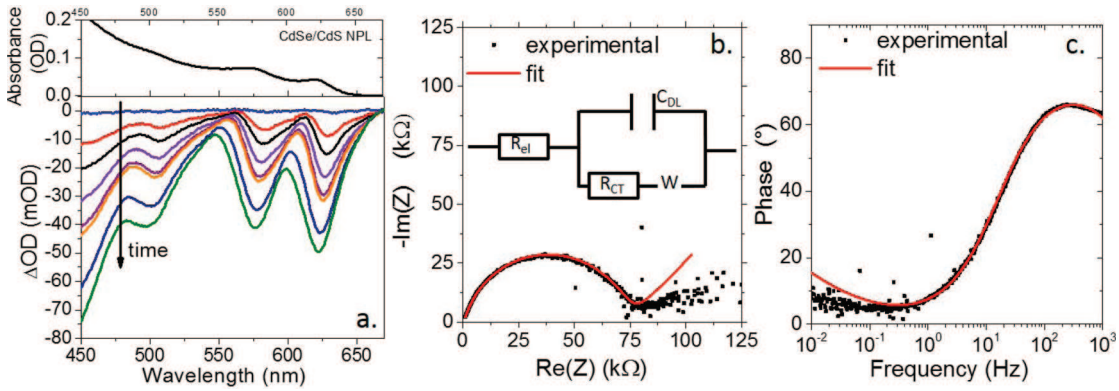

Figure 3. (a) Top: absorption spectrum of the CdSe/CdS film. Bottom: the change in the absorption at different times under a 2 V gate bias. (b) Nyquist plot (imaginary part as a function of the real part) of the impedance of a CdSe/CdS film. The data are fitted using the proposed equivalent circuit given in inset. (d) Phase plot associated with the impedance plot. For panels b and c, a 2 V DC gate bias is modulated by a 1 mV AC bias.

Finally, we add a diffusion term W (Warburg diffusion impedance) to model the tail occurring at low frequency. In general, W is expressed as $W = (A/\sqrt{w}) + (A/(j\sqrt{w}))$, where A is an amplitude that in our case is 6 ± 2 kΩ·s$^{-1/2}$. This term leads to a 45° slope in the impedance curve and accounts for the diffusion of the ion into the electrolyte. However, we typically observe a much smaller slope, which comes as a deviation compared with the equivalent circuit modeling; see Figure 3b. We attribute this deviation to a second source of diffusion-limited process, which is the percolation of the Li^+ ions within the nanoparticle film. This diffusion is known to be sensitive to the presence of voids, which leave space for the ions to diffuse.[23] In a previous study we demonstrated the fact that the gating was quite sensitive to the packing of the NPL.[4] In particular, the NPL core tends to stack, which prevents the Li^+ percolation and makes the gating ineffective. We conducted a study of the CdSe/CdS NPL film morphology by extracting a layer of the film using focused ion beam processing. The film is then further characterized using SEM (Figure 4a) and TEM (Figure 4b,c). We observe that despite the cubic aspect of the NPL the film is full of voids with a broad size distribution between 1 and 50 nm. These voids are responsible for the gating, even for thick films (up to micrometers). The less effective gating obtained with the CdTe NPL compared with the CdSe/CdS may not result from the material but instead from the difference in lateral size. The CdTe NPLs typically have a lateral extension >100 nm, and this makes the percolation path for the cation more complex.

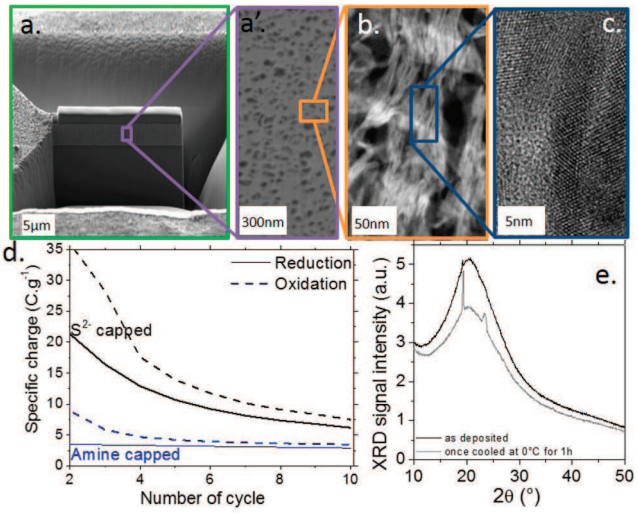

Figure 4. (a,a′) SEM images of a slice of CdSe/CdS film cut using FIB. (b,c) TEM images of the same film as panel a. (d) Apecific charge for film of CdSe/CdS NPL capped with butylamine and S^{2-} extracted from the cyclic voltammetry. (e) XRD for as-prepared electrolyte and after 1 h at 0 °C.

3.3. Structural Properties of the Film. A striking feature related to this gating process is its dependence on the surface chemistry. As previously stated, the ligand exchange was first motivated by the enhancement of the interparticle coupling; however, cyclic voltammetry (CV, see Figure S13) showed significant variations with different capping ligands; see Figure 4d.

The integrated charge extracted from the CV curve (see Figure 4d) is significantly higher for atomically short (S^{2-}) passivation by a factor 5 to 10. This latter property remains true even after several cycles. Over the first cycles, the reduction of undesired organic species in the solution leads to a large asymmetry between the oxidation and reduction current. The overall increase in the injected charge into the film results from the higher availability of nanocrystal surface, which leads as a response to an easier tunnel injection of the electrons into the quantum states by the electrodes. This is consistent with the use of similar nanoparticle surface chemistries in the field of batteries.[24]

In the last section we discuss the temperature dependence of this electrolyte gating and its stability. Electrolyte gating generally may lead to some charge fluctuation even under constant potential. To limit this fluctuation, it is useful to freeze the electrolyte by cooling the sample below the melting point of the matrix. In the case of ion gel gating the higher viscosity of the matrix limits this fluctuation. While at room temperature (20 °C) we observe an efficient gating, the charge injection is completely stopped already at 0 °C. In the PEG matrix, the Li^+ diffuses under a solvated form where an ether crown is formed, and its rearrangement allows the ionic displacement. At 0 °C the PEG matrix freezes, as observed on the XRD diffractogram (see Figure 4e), while the latter presents no fine structure at room temperature. The formation of crystallines zones prevents the rearrangement of the ether crown and the ionic displacement is suppressed. Having a polymer electrolyte with a freezing temperature close to room temperature consequently reduces the charge fluctuation compared with electrolyte with a lower freezing point.

4. CONCLUSIONS

We propose a versatile method for electrolyte gating of NPL and nanocrystal films. The obtained devices, almost solid thin solids, are air operable. We provided evidence that the charges are indeed injected in the quantum states of the nanocrystals. This efficient gating is made possible by the large porosity of the NPL film with large voids letting the ions percolate even through thick films of NPL.

■ ASSOCIATED CONTENT

Supporting Information

The Supporting Information is available free of charge on the ACS Publications Web site at DOI: The Supporting Information is available free of charge on the ACS Publications website at DOI: 10.1021/acs.jpcc.5b05296.

Additional data giving details of the material synthesis and complementary information related to the transistor characterization. (PDF)

■ AUTHOR INFORMATION

Corresponding Authors

*E.L.: E-mail: Emmanuel.Lhuillier@insp.upmc.fr.

*B.D.: E-mail: benoit.dubertret@espci.fr.

Present Address

⊥CNRS, UMR 7588, Institut des Nano-Sciences de Paris (INSP), 4 place Jussieu, 75005 Paris, France.

Notes

The authors declare no competing financial interest.

■ ACKNOWLEDGMENTS

B.D. thanks ANR (grant SNAP) for funding. We are grateful to the METSA network and the CLYM laboratory for performing imaging of NPL film. We thank Sean Keuleyan for the corrections of the manuscript.

■ REFERENCES

(1) Lhuillier, E.; Pedetti, S.; Ithurria, S.; Nadal, B.; Heuclin, H.; Dubertret, B. *2D* Colloidal Metal Chalcogenides Semiconductors: Synthesis, Spectroscopy and Applications. *Acc. Chem. Res.* **2015**, *48*, 22.

(2) Ithurria, S.; Tessier, M. D.; Mahler, B.; Lobo, R. P. S. M.; Dubertret, B.; Efros, Al. L. Colloidal nanoplatelets with two-dimensional electronic structure. *Nat. Mater.* **2011**, *10*, 936−941.

(3) Ithurria, S.; Dubertret, B. Quasi 2D Colloidal CdSe Platelets with Thicknesses Controlled at the Atomic Level. *J. Am. Chem. Soc.* **2008**, *130*, 16504.

(4) Lhuillier, E.; Pedetti, S.; Ithurria, S.; Heuclin, H.; Nadal, B.; Robin, A.; Patriarche, G.; Lequeux, N.; Dubertret, B. Electrolyte Gated Field Effect Transistor to Probe the Surface Defects and Morphology in Films of Thick CdSe Colloidal Nanoplatelets. *ACS Nano* **2014**, *8*, 3813.

(5) Lhuillier, E.; Robin, A.; Ithurria, S.; Aubin, H.; Dubertret, B. Electrolyte gated colloidal nanoplatelets based phototransistor and its use for bicolor detection. *Nano Lett.* **2014**, *14*, 2715.

(6) Lhuillier, E.; Dayen, J. F.; Thomas, D. O.; Robin, A.; Doudin, B.; Dubertret, B. Nanoplatelets bridging a nanotrench: a new architecture for photodetectors with increased sensitivity. *Nano Lett.* **2015**, *15*, 1736−1742.

(7) Wang, C.; Shim, M.; Guyot-Sionnest, P. Electrochromic nanocrystal quantum dots. *Science* **2001**, *291*, 2390.

(8) Vanmaekelbergh, D.; Houtepen, A. J.; Kelly, J. J. Electrochemical gating: a method to tune and monitor the (opto) electronic properties of functional materials. *Electrochim. Acta* **2007**, *53*, 1140.

(9) Guyot-Sionnest, P. Charging colloidal quantum dots by electrochemistry. *Microchim. Acta* **2008**, *160*, 309−314.

(10) Germeau, A.; Roest, A. L.; Vanmaekelbergh, D.; Allan, G.; Delerue, C.; Meulenkamp, E. A. Optical Transitions in Artificial Few-Electron Atoms Strongly Confined inside ZnO Nanocrystals. *Phys. Rev. Lett.* **2003**, *90*, 097401.

(11) Kang, M. S.; Lee, J.; Norris, D. J.; Frisbie, C. D. High carrier densities achieved at low voltages in ambipolar PbSe nanocrystal thin-film transistor. *Nano Lett.* **2009**, *9*, 3848.

(12) Kang, M. S.; Sahu, A.; Norris, D. J.; Frisbie, C. D. Size-dependent electrical transport in CdSe nanocrystal thin films. *Nano Lett.* **2010**, *10*, 3727.

(13) Kang, M. S.; Sahu, A.; Frisbie, C. D.; Norris, D. J. Influence of Silver Doping on Electron Transport in Thin Films of PbSe Nanocrystals. *Adv. Mater.* **2013**, *25*, 725.

(14) Kang, M. S.; Sahu, A.; Norris, D. J.; Frisbie, C. D. Size-and temperature-dependent charge transport in PbSe nanocrystal thin films. *Nano Lett.* **2011**, *11*, 3887.

(15) Bisri, S. Z.; Piliego, C.; Yarema, M.; Heiss, W.; Loi, M. A. Low driving voltage and high mobility ambipolar field-effect transistors with PbS colloidal nanocrystals. *Adv. Mater.* **2013**, *25*, 4309.

(16) Chen, O.; Chen, X.; Yang, Y.; Lynch, J.; Wu, H.; Zhuang, J.; Cao, Y. C. Synthesis of Metal−Selenide Nanocrystals Using Selenium Dioxide as the Selenium Precursor. *Angew. Chem., Int. Ed.* **2008**, *47*, 8638.

(17) Pedetti, S.; Nadal, B.; Lhuillier, E.; Mahler, B.; Bouet, C.; Abécassis, B.; Xu, X.; Dubertret, B. Optimized synthesis of CdTe nanoplatelets and photoresponse of CdTe nanoplatelets films. *Chem. Mater.* **2013**, *25*, 2455.

(18) Nag, A.; Kovalenko, M. V.; Lee, J. S.; Liu, W.; Spokoyny, B.; Talapin, D. V. *Metal-free inorganic ligands for colloidal nanocrystals:* S^{2-}, HS^{-}, Se^{2-}, HSe^{-}, Te^{2-}, HTe^{-}, TeS_3^{2-}, OH^{-}, *and* NH_2^{-} *as surface ligands. J. Am. Chem. Soc.* **2011**, *133*, 10612.

(19) Ithurria, S.; Talapin, D. V. Colloidal Atomic Layer Deposition (c-ALD) using Self-Limiting Reactions at Nanocrystal Surface Coupled to Phase Transfer between Polar and Nonpolar Media. *J. Am. Chem. Soc.* **2012**, *134*, 18585.

(20) Boehme, S. C.; Azpiroz, J. M.; Aulin, Y. V.; Grozema, F. C.; Vanmaekelbergh, D.; Siebbeles, L. D. A.; Infante, I.; Houtepen, A. J. Density of Trap States and Auger-mediated Electron Trapping in CdTe Quantum-Dot Solids. *Nano Lett.* **2015**, *15*, 3056.

(21) Yuan, H.; Shimotani, H.; Ye, J.; Yoon, S.; Aliah, H.; Tsukazaki, A.; Kawasaki, M.; Iwasa, Y. Electrostatic and Electrochemical Nature of Liquid-Gated Electric-Double-Layer Transistors Based on Oxide Semiconductors. *J. Am. Chem. Soc.* **2010**, *132*, 18402−18407.

(22) Lu, M.; Beguin, F.; Frackowiak, E. In *Supercapacitors: Materials, Systems and Applications*; Wiley: New York, 2013.

(23) Boehme, S. C.; Wang, H.; Siebbeles, L. D. A.; Vanmaekelbergh, D.; Houtepen, A. J. Electrochemical Charging of CdSe Quantum Dot Films: Dependence on Void Size and Counterion Proximity. *ACS Nano* **2013**, *7*, 2500.

(24) Oszajca, M. F.; Bodnarchuk, M. I.; Kovalenko, M. V. Precisely Engineered Colloidal Nanoparticles and Nanocrystals for Li-Ion and Na-Ion Batteries: Model Systems or Practical Solutions? *Chem. Mater.* **2014**, *26*, 5422−5432.